Vol. 39, No. 1 (2017) 82-89

Tribology in Industry

www.tribology.fink.rs

RESEARCH

# Mixed Lubrication Solution of Dynamically Loaded Radial Slide Bearings

P. Novotny[a]

[a] *Brno University of Technology, Technicka 2, 616 69, Brno, Czech Republic.*

Keywords:

*Elastic deformations*
*Asperity*
*Contact*
*Hydrodynamics*
*Algorithm*

Corresponding author:

*Pavel Novotny*
*Brno University of Technology*
*Technicka 2, 616 69, Brno,*
*Czech Republic.*
*E-mail: novotny.pa@fme.vutbr.cz*

A B S T R A C T

*A solution of radial slide bearing dynamics and tribology incorporating the influences of real surface roughness contacts or the influence of surface roughness on bearing lubrication is presented in this paper. Finite difference method for Reynolds equation discretization, finite element method for calculation of elastic deformations, Gauss-Seidel's method for iterative solution of discretized equations or Newmark's algorithm are the methods employed in the proposed solution approach. The coupled structural-fluid solver considering mixed lubrication conditions of the radial bearings is the result. The proposed algorithms are presented for highly loaded radial slide bearing of internal combustion engine.*



## 1. INTRODUCTION

This work deals with the development of effective algorithms for modelling the fluid-structure problem as it can be seen for example in radial slide bearings. In the technical literature, the problems of slide bearing modelling (interaction of rigid part and a thin fluid layer) are frequently published and described in quite a detail e.g. references [1, 2, 3], they are studied qualitatively for more than a century. The theory of lubrication is based on Reynolds equation in some form. In general, this nonlinear partial differential equation has been experimentally validated. The Reynolds equation assumes some simplifications defined for example in [3].

The Reynolds equation has to be supplemented by the cavitation equation. Cavitation phenomena, in general, usually occur in the regions of diverging gaps filled by liquid under sub-ambient pressure. These very low pressures cause a transformation of liquid to liquid-gas mixture. Numerous cavitation algorithms have been proposed over time. The basic ones, like Half-Sommerfeld or Reynolds, can be used. A more sophisticated approach was introduced by Jacobsson and Floberg [4]. Elrod [5] introduced a new cavitation algorithm using only a single equation for the whole lubrication region without the need to locate cavitation boundaries. These algorithms are, in general, mass conservative and if thermal effects are to be considered, there is definitely a need to use these or similar approaches. However, if the

main required result is the pressure distribution in oil film, then the numerically simple Reynolds description of cavitation can be used.

Structural elastic deformations of a pin or a shell have a significant influence on a slide bearing behaviour. However these effects are far more important if the bearing is highly loaded. Today, when highly turbocharged engines are in operation, the elastic deformations have to be considered already in the phase of the development process. Computational approaches considering elastic deformations complicate the numerical solution and are not frequently included in commercial products. Brief overview of an elasto-hydrodynamic solution presents, e.g. Thomas [6], Caika [7], Javorova [8] or Okamoto [9]. The publishing of exclusively general procedures is the main disadvantage of similar technical contributions, while detailed instructions for the numerical solution is not presented often.

If very thin oil film thickness is reached, the influence of surface roughness on lubrication has to be taken into consideration. Special correction factors [11], so-called flow factors, are proposed. The flow factors modify the Reynolds equation to the form of:

$$\frac{\partial}{\partial x}\left(\phi_x \frac{\rho h^3}{12\eta}\frac{\partial p}{\partial x}\right)+\frac{\partial}{\partial z}\left(\phi_z \frac{\rho h^3}{12\eta}\frac{\partial p}{\partial z}\right)- \frac{U}{2}\frac{\partial(\rho h_A)}{\partial x}-\frac{\partial(\rho h_A)}{\partial t}-\frac{U}{2}\sigma\frac{\partial \phi_s}{\partial x}=0 \quad (1)$$

Numerical calculation of flow factors proposed by Marsalek [10] is used in this work. This approach covers arbitrary directionally oriented surfaces. If directionally non-oriented surfaces with normal distribution are considered, then the approach by Patir and Cheng [11] or Arcoumanis [12] can be applied.

Reynolds equation requires the definition of oil film thickness. The oil film thickness consists of several components, i.e. the component reflecting the the clearance between the rigid pin and shell – $h_R$. The second component is the elastic deformation $h_E$, while the third component $h_I$ includes irregularities of the pin or the shell from an ideal cylinder (initial deformations).

Friction losses are one of the most important results and therefore the definition of shear stress including the influence of surface roughness is defined as:

$$\tau = \pm\phi_{fp}\frac{h}{2}\frac{\partial \overline{p}}{\partial x}-(\phi_f+\phi_{fs})\frac{\eta U}{h} \quad (2)$$

A more complex simulation strategy requires the inclusion of contact forces into the solution. An approach proposed by Greenwood and Tripp [13] is frequently used, but there are some limitations. The contact behaviour is considered as elastic, which is not absolutely true, and the surfaces have to be considered as surfaces with normal distribution of roughness peak heights. The approach by Greenwood and Tripp also presumes constants describing surface roughness obtained by experimental technique from the late 1980's. Considering all the disadvantages of the Greenwood and Tripp contact model, a more advanced approach defined by Pasaribu and Schipper [14] is used in this work. Successful application of Finite Element modelling on a description of surface contacts presents also Amor [15]. The selection of the contact model is based on the study by Marsalek [10].

Obtaining the surface characteristics is a very important task. The surface structures can be scanned from existing components or they can be generated using special algorithms on the base of typical marks of manufacturing processes, like turning or grinding operations. Both of the approaches are also presented by Marsalek [10].

## 2. MAIN OBJECTIVES OF DEVELOPMENT ACTIVITIES

The main objective of this work is to propose a new, complex, robust and time-effective algorithm considering significant influences on dynamically loaded slide bearings directly usable in industrial tribology. Numerical algorithms, as a computer code, are the main results. The code includes mixed lubrication solver covering all significant influences of lubrication.

The considered influences are variable oil properties in dependency on pressure and temperature, cavitation of oil, elastic deformations of structures, influence of directionally oriented surface microstructures

on lubrication; surface roughness contacts, oil feeding influences and initial deformations of a shell or a pin.

Authors' objective is also to describe numerical approaches in more detail and also to enable other researchers use these approaches. All the numerical approaches presented are integrated into a program BearDYN developed by the authors. Proposed methods are applied on a highly loaded slide bearing of the connecting rod big eye of an internal combustion engine (ICE).

## 3. THEORY BACKGROUND

### 3.1. Fluid Region Description

Modified Reynolds equation (1) is discretised by Finite Difference Method (FDM), but before this process the Reynolds equation is transformed into a non-dimensional form. This form presents advantages for the numerical solution. The substitutions are introduced as:

$$\begin{aligned} H &= \frac{h}{R-r} = \frac{h}{c} \qquad \bar{\rho} = \frac{\rho}{\rho_0} \qquad \bar{\eta} = \frac{\eta}{\eta_0} \\ \varphi &= \frac{x}{R} \qquad Z = \frac{z}{B} \qquad \upsilon = \frac{B}{R} = \frac{2B}{D} \\ P &= \frac{pc^2}{12R^2\eta_0} \qquad \bar{U}_n = \frac{U_n}{c} = \dot{H} \qquad \bar{U} = \frac{U}{2R} \\ \xi_x &= \phi_x \frac{\bar{\rho}H^3}{\bar{\eta}} \qquad \xi_x = \phi_x \frac{\bar{\rho}H^3}{\bar{\eta}} \qquad \bar{\sigma} = \frac{\sigma}{c\rho_0} \end{aligned} \tag{3}$$

If equations (3) are substituted into equation (1), the final form of the non-dimensional Reynolds equation is:

$$\begin{aligned} &\frac{\partial}{\partial\varphi}\left(\xi_x \frac{\partial P}{\partial\varphi}\right) + \frac{1}{\upsilon^2}\frac{\partial}{\partial Z}\left(\xi_z \frac{\partial P}{\partial Z}\right) - \bar{U}\frac{\partial(\bar{\rho}H_A)}{\partial\varphi} \\ &-\left(\dot{\bar{\rho}}H_A + \bar{\rho}\dot{H}_A\right) - \bar{U}\bar{\sigma}\frac{\partial\phi_s}{\partial\varphi} = 0 \end{aligned} \tag{4}$$

where $H_A$ is the locally averaged oil film thickness. The value of the locally averaged thickness is determined from surface statistics or is calculated based on the approach by Patir a Cheng [11].

### 3.2. Structural Region Description

In general the dynamic behaviour of elastic structures is described by the equation of motion. Finite Element Method (FEM) is employed to discretise pin and shell structures and to compute condensed matrices. In this case the discretised equation of the motion is:

$$\mathbf{M}\ddot{\mathbf{h}}_{\mathbf{E}}^{k} + \mathbf{B}\dot{\mathbf{h}}_{\mathbf{E}}^{k} + \mathbf{K}\mathbf{h}_{\mathbf{E}}^{k} = \mathbf{F}^{k} \tag{5}$$

Then relative elastic deformation reads as:

$$\mathbf{H}_{\mathbf{E}}^{k} = \frac{\mathbf{h}_{\mathbf{E}}^{k}}{c} = \frac{1}{c}\mathbf{A}_{\mathbf{F}}\mathbf{Q}^{k} = \mathbf{A}_{\mathbf{F}}\mathbf{Q}_{\mathbf{R}}^{k}, \tag{6}$$

where $Q_R$ is the relative complex load matrix and it can be computed as:

$$\begin{aligned} \mathbf{Q}_{\mathbf{R}}^{k} &= \frac{12A_0R^2\eta_0}{c^3}\mathbf{P}_{\mathbf{T}} \\ &+\mathbf{M}\left[\frac{1}{\beta\Delta t^2}\mathbf{H}_{\mathbf{E}}^{k} + \frac{1}{\beta\Delta t}\dot{\mathbf{H}}_{\mathbf{E}}^{k} + \left(\frac{1}{2\beta}-1\right)\ddot{\mathbf{H}}_{\mathbf{E}}^{k}\right] \\ &+\mathbf{B}\left[\frac{\gamma}{\beta\Delta t}\mathbf{H}_{\mathbf{E}}^{k} + \left(\frac{\gamma}{\beta}-1\right)\dot{\mathbf{H}}_{\mathbf{E}}^{k} + \left(\frac{\gamma}{2\beta}-1\right)\Delta t\ddot{\mathbf{H}}_{\mathbf{E}}^{k}\right] \end{aligned} \tag{7}$$

where $P_T$ is the total pressure consisting of hydrodynamic pressure and contact pressure. Matrix $A_F$ presents the complex compliancy matrix and can be calculated as:

$$\mathbf{A}_{\mathbf{F}} = \left(\frac{1}{\beta\Delta t^2}\mathbf{M} + \frac{\gamma}{\beta\Delta t}\mathbf{B} + \mathbf{K}\right)^{-1} \tag{8}$$

Matrices M and K are obtained by commercial FEM software ANSYS. Proportional damping is applied on the structure, a damping matrix is proposed as

$$\mathbf{B} = \alpha_p\mathbf{M} + \beta_p\mathbf{K} \tag{9}$$

Matrix of the relative velocity of elastic deformation $\dot{\mathbf{H}}_{\mathbf{E}}$ is obtained by Newmark's algorithm using previous time step values as

$$\begin{aligned} \dot{\mathbf{H}}_{\mathbf{E}}^{k} &= \frac{\gamma}{\beta\Delta t}(\mathbf{H}_{\mathbf{E}}^{k} - \mathbf{H}_{\mathbf{E}}^{k-1}) - \left(\frac{\gamma}{\beta}-1\right)\dot{\mathbf{H}}_{\mathbf{E}}^{k-1} \\ &-\left(\frac{\gamma}{2\beta}-1\right)\Delta t\ddot{\mathbf{H}}_{\mathbf{E}}^{k-1} \end{aligned} \tag{10}$$

Matrix of relative acceleration of the elastic deformation is

$$\begin{aligned} \ddot{\mathbf{H}}_{\mathbf{E}}^{k} &= \frac{1}{\beta\Delta t^2}(\mathbf{H}_{\mathbf{E}}^{k} - \mathbf{H}_{\mathbf{E}}^{k-1}) - \frac{1}{\beta\Delta t}\dot{\mathbf{H}}_{\mathbf{E}}^{k-1} \\ &-\left(\frac{1}{2\beta}-1\right)\ddot{\mathbf{H}}_{\mathbf{E}}^{k-1} \end{aligned} \tag{11}$$

### 3.3. Solution of Oil Film Pressure Distribution

For each time step the components $h_I$ of oil film thickness remains constant. The component $h_R$ is calculated based on pin position changes during a solution of force equilibrium. The elastic component of oil film thickness $h_E$ is updated every iteration within a time step and during a solution of Reynolds equation. The relative oil film thickness reads as:

$$\mathbf{H} = \frac{1}{c}\left(\mathbf{h_R} + \mathbf{h_E} + \mathbf{h_I}\right) = \mathbf{H_R} + \mathbf{H_E} + \mathbf{H_I} \tag{12}$$

The rlative velocity of oil film thickness $\dot{\mathbf{H}}$ reads as:

$$\dot{\mathbf{H}} = \frac{\mathbf{U_N}}{c} + \dot{\mathbf{H}}_\mathbf{E} = \dot{\mathbf{H}}_\mathbf{R} + \dot{\mathbf{H}}_\mathbf{E} \tag{13}$$

and the relative acceleration of oil film thickness $\ddot{\mathbf{H}}$ reads as:

$$\ddot{\mathbf{H}} = \ddot{\mathbf{H}}_\mathbf{R} + \ddot{\mathbf{H}}_\mathbf{E} \tag{14}$$

Again, the elastic component of oil film thickness velocity $\dot{\mathbf{H}}_\mathbf{E}$ is updated every iteration within a time step. The matrix of derivative of dimensionless density $\dot{\bar{\boldsymbol{\rho}}}$ can be computed as follows:

$$\dot{\bar{\boldsymbol{\rho}}}^k = \frac{1}{\Delta t}(\bar{\boldsymbol{\rho}}^k - \bar{\boldsymbol{\rho}}^{k-1}). \tag{15}$$

### 3.4. Numerical Solution of Reynolds Equation

Reynolds equation presents an unsteady nonlinear differential equation of second order and the Finite Difference Method (FDM) is employed for discretisation. The equation (4) is considered nonlinear and therefore some more advanced strategy has to be incorporated. Newton-Raphson (NR) procedure is used in this work. Residuum and Jacobian have to be defined to meet the requirements of the NR procedure. The residuum in the node *i, j* is defined as:

$$\begin{aligned} r_{i,j} = & \\ & + \frac{\xi_{xi+1/2,j}P_{i+1,j} - (\xi_{xi+1/2,j} + \xi_{xi-1/2,j})P_{i,j} + \xi_{xi-1/2,j}P_{i-1,j}}{h_\varphi^2} \\ & + \frac{\xi_{zi,j+1/2}P_{i,j+1} - (\xi_{zi,j+1/2} + \xi_{xi,j-1/2})P_{i,j} + \xi_{xi,j-1/2}P_{i,j-1}}{h_Z^2} \\ & - \bar{U}_{i,j}\frac{1.5\bar{\rho}_{i,j}H_{Ai,j} - 2.0\bar{\rho}_{i-1,j}H_{Ai-1,j} + 0.5\bar{\rho}_{i-2,j}H_{Ai-2,j}}{h_\varphi} \\ & - \bar{U}_{i,j}\bar{\sigma}_{i,j}\frac{\phi_{si+1,j} - \phi_{si-1,j}}{2h_\varphi} - \dot{\bar{\rho}}_{i,j}H_{Ai,j} - \bar{\rho}_{i,j}\dot{H}_{Ai,j} \end{aligned} \tag{16}$$

and Jacobian incorporating elastic deformations reads as:

$$\begin{aligned} J_{i,j} = & \\ & - \frac{(\xi_{xi+1/2,j} + \xi_{xi-1/2,j})}{h_\varphi^2} - \frac{1}{\upsilon^2}\frac{(\xi_{zi,j+1/2} + \xi_{zi,j-1/2})}{h_Z^2} \\ & - \bar{U}_{i,j}\frac{1.5\bar{\rho}_{i,j}^k C_0 - 2\bar{\rho}_{i-1,j}^k C_1 + 0.5\bar{\rho}_{i-2,j}^k C_2}{h_\varphi} \\ & - \dot{\bar{\rho}}_{i,j}^k C_0 - \frac{1}{\Delta t}\bar{\rho}_{i,j}^k C_0 \end{aligned} \tag{17}$$

(12)

Set of constants, generally written $C_\beta$, introduces a member of complex compliance matrix in distance $\psi$ from the main matrix diagonal. It can be defined as:

(13)

$$C_\psi = C_{i+m(j-1),i+m(j-1)-\psi} \tag{18}$$

The discretised equation is solved by Gauss-Seidel iterative method incorporating Successive Over-Relaxation (SOR) strategy. The updated pressure in node *i, j* is then given by:

(14)

$$P_{i,j}^{k,s+1} = P_{i,j}^{k,s} - \omega_{SOR}\frac{r_{i,j}}{J_{i,j}} \tag{19}$$

Equation (36) has to be supplemented by the following cavitation condition:

$$P_{i,j} = P_{cav} \quad if \quad P_{i,j} < P_{cav} \tag{20}$$

which continually limits pressures up to cavitation pressure during the iterative process. Moreover, a condition defining values of pressures on oil channels and grooves is added:

$$P_{i,j} = P_G \tag{21}$$

### 3.5. Modelling the Surface Roughness Contacts

An elasto-plastic deterministic contact model proposed by Pasaribu & Schipper [13] is used in this work. This computational model takes into account all three states of material behaviour – fully elastic, elasto-plastic, and fully plastic. The principle of this approach is to calculate contact force driven by the value of deflection (penetration) $\delta_R$ of contact bodies. The theory can be found in [14].

(16)

The integral value of contact pressure in a node is calculated as the sum of contact forces divided by the contact area of neighbouring nodes using trapeze rule:

$$P_{ci,j} = \frac{1}{8}\left( 4\frac{F_{ci,j}}{A_{ci,j}} + \frac{F_{ci+1,j}}{A_{ci+1,j}} + \frac{F_{ci-1,j}}{A_{ci-1,j}} + \frac{F_{ci,j+1}}{A_{ci,j+1}} + \frac{F_{ci,j-1}}{A_{ci,j-1}} \right) \quad (22)$$

## 4. APPLICATION OF PROPOSED MIXED LUBRICATION SOLUTION

Computational models are applied to the slide bearing of the connecting rod big eye of a spark ignition (SI) aircraft engine. The engine relative loading is not too high compared to contemporary highly turbocharged diesel engines. However, the aluminium alloys used as material of connecting rod introduce significant issues in the area of bearing lubrication. Table 1 presents selected operating data and parameters of the engine.

**Table 1.** Selected operating data and parameters of the slide bearing.

| | |
|---|---|
| Operating engine speed [min$^{-1}$] | 2700 |
| Peak combustion pressure [MPa] | 7 |
| Material of a connecting rod | Aluminium alloy |
| SAE type of lube oil | 15W-40 |
| Bearing inlet oil temperature [°C] | 70 |

### 4.1. Determination of Real Slide Bearing Surface Roughness

A bearing shell of a connecting rod of the target engine has been scanned in ten different places and the resultant scans have been statistically evaluated.

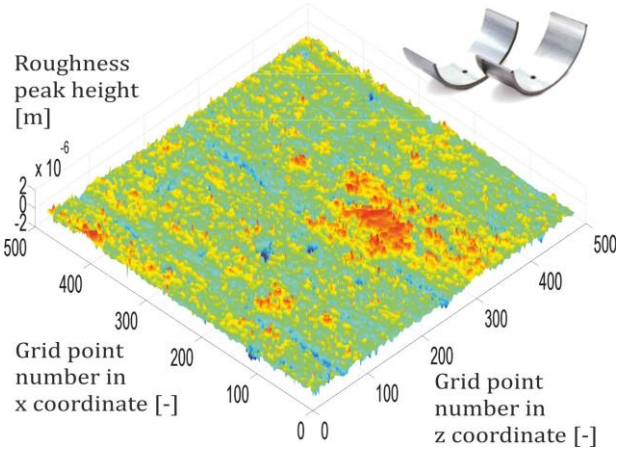


**Fig. 1.** Scanned surface of the bearing shell.

Averaged flow factors, contact pressures and contact areas in dependency on ratio of middle surface distance to combined surface roughness *(h/σ)* are the main results that will be used for the calculations of hydrodynamic and contact pressures. Figure 1 presents the scanned surface of the bearing shell. Scanned area is 118x118 μm.

(22)

Scanned surface demonstrates significant anisotropy of roughness, therefore the flow factors in *x* and *z* show differences. The resulting flow factors are presented in Fig. 2.

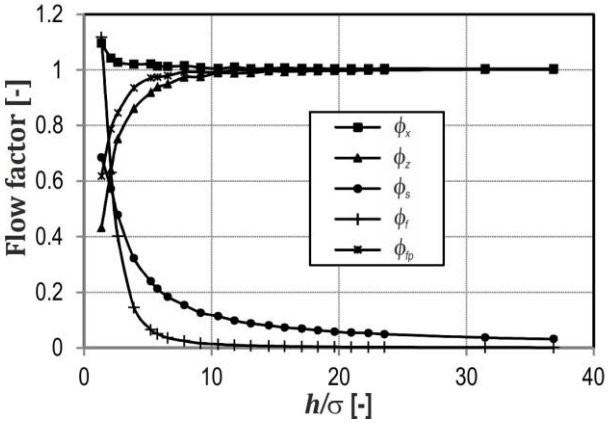


**Fig. 2.** Evaluated flow factors of the scanned surface

Figure 3 presents the evaluated surface roughness contact pressures vs. ratio of distance of middle surfaces to combined surface roughness. The results are averaged from 10 different places.

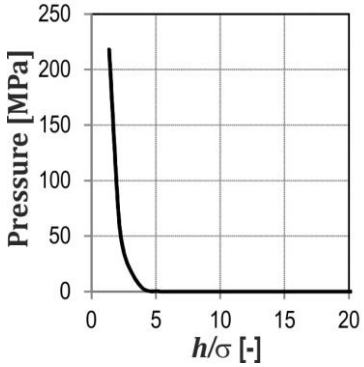


**Fig. 3.** Evaluated averaged contact pressure of the scanned surface

### 4.2. Comparison of Connecting Rod Designs

The proposed algorithms, by means of code BearDYN, are applied to a verification of slide bearings of big eye connecting rod designs. This includes calculations of slide bearing performances for base and modified designs.
The proposed design modifications are limited by diameter and width of new crankshaft crank pin. Therefore, the bearing diameter and width

are fixed, without any possibilities to change them. The bearing clearance is one of free parameters that can be modified. Material, lube oil and main slide bearing dimensions for both designs are presented in Table 2.

**Table 2.** Slide bearing description for base and modified designs of connecting rod big eye.

| | Base design | Modified design |
|---|---|---|
| Material of a shell (prevailing) | Steel | Steel |
| Motor lube oil (SAE) | 15W-40 | 10W-40 |
| Engine speed [min$^{-1}$] | 2750 | 2750 |
| Bearing diameter [mm] | 42 | 42.5 |
| Bearing width [mm] | 30 | 20 |
| Shell thickness [mm] | 3 | 1.5 |

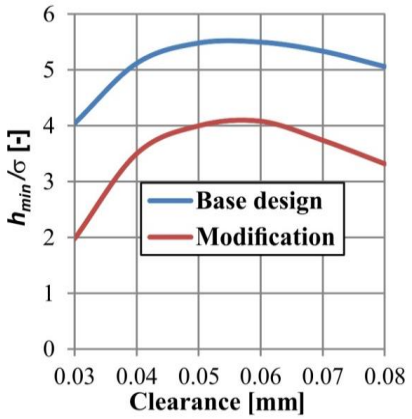


**Fig. 4.** Ratio of minimal oil film thickness and combined surface roughness.

Figure 4 shows a ratio of bearing minimal oil film thickness and combined surface roughness ($h_{min}/\sigma$) of pin and shell surfaces.

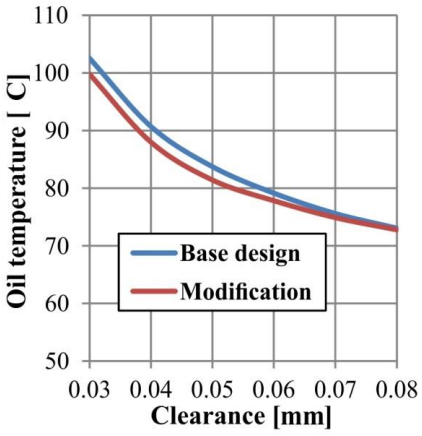


**Fig. 5.** Averaged oil film temperatures vs. a bearing clearance.

The modified design requires restriction of the bearing clearance range to avoid contacts of surface peaks. The contacts of surface peaks are connected with increased wear.

Averaged oil film temperature of the bearings is an important result (Fig. 5) which does not show any significant differences for modified design.

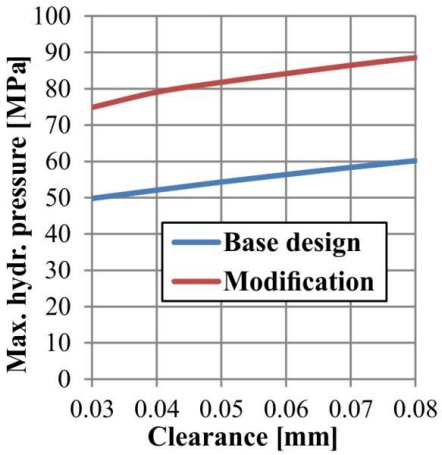


**Fig. 6.** Maximal hydrodynamic pressures vs. a bearing clearance.

Figure 6 presents maximal hydrodynamic pressures in bearing oil film vs. a bearing clearance. Fatigue life of slide bearing components (pin and shell) can be evaluated from the values of hydrodynamic and contact pressures in dependency on time.

## 5. SOLUTION APPROACH SUMMARY

Significant differences can be found among the algorithms proposed in the past. Hydrodynamic models (HD) introduce higher loading capacity than elasto-hydrodynamic (EHD) models. It is caused by extremely high values of hydrodynamic pressures in oil film for high bearing eccentricities. Neither of them considers surface roughness contacts. The solution is to use the more complex model considering hydrodynamics, contacts and elastic structures (REHD) proposed by the authors.

In general, the models which do not consider the elastic deformations overestimate the values of hydrodynamic pressures. This effect can cause significant inaccuracy, if fatigue of bearing components is analysed. The results show that the elastic deformations have to be considered for the highly loaded bearings of internal combustion engines, especially in the case of main journal or connecting rod bearings.

The influence of rough surfaces on bearing lubrication presents a significant impact mainly on the values of bearing friction losses, described by the flow factor theory in the case of hydrodynamics, which is in this work presented via equations (2) and (5). It is evident that the modern computational models should incorporate influences of rough surfaces in some way, otherwise the estimation of hydrodynamic power loss and the warm up of the oil film can be inaccurate.

## 6. CONCLUSIONS

The aim of the work is to introduce a complex, robust and well described methodology for numerical solutions and analyses of dynamically loaded slide bearings considering elastic deformations and surface roughness effects. The proposed REHD computational model has been applied on a highly loaded bearing of a connecting rod of a SI engine. Therefore the presence of some highly important phenomena can be assumed, like elastic deformations or rough surface influences. In case a less loaded bearing is chosen, these effects would be less significant.

The proposed algorithm enables engineers or researches who are not highly specialized in numerical techniques to carry out simulations without buying expensive commercial simulation tools.

## Acknowledgement

Outputs of this project, named NETME CENTRE PLUS (LO1202), were created with financial support from the Ministry of Education, Youth and Sports of the Czech Republic under the program supporting research, experimental development and innovation: "National Sustainability Programme I." Authors gratefully acknowledge this support.

## Nomenclature

| | |
|---|---|
| $c$ | bearing clearance ($c = R - r$) [m] |
| $d$ | pin diameter [m] |
| $e$ | pin eccentricity [m] |
| $h$ | oil film thickness [m] |
| $h_A$ | locally averaged oil film thickness [m] |
| $h_R$ | rigid component of oil film thickness [m] |
| $h_E$ | elastic component of oil film thickness [m] |
| $h_A$ | locally averaged oil film thickness [m] |
| $h_\varphi$, $h_z$ | steps in coordinates [-] |
| $p$ | pressure [Pa] |
| $r$ | pin radius [m] |
| $t$ | time [s] |
| $x$, $y$, $z$ | coordinates [m] |
| $A_0$ | area of FDM element [m$^2$] |
| $A_c$ | contact areas [m$^2$] |
| $B$ | bearing width [m] |
| $C_\psi$ | member of complex compliance matrix [N$^{-1}$m] |
| $D$ | shell diameter [m] |
| $E'$ | combined Young's modulus [P] |
| $F_c$ | contact force [N] |
| $H$ | relative oil film thickness [-] |
| $H_{i,j}^{k,s}$ | discrete value of relative oil film thickness at node $i$, $j$ of time step $k$ at iteration $s$ [-] |
| $H_A$ | locally averaged relative oil film thickness [-] |
| $H_E$ | relative elastic deformation [-] |
| $H_I$ | pin or shell cylindrical irregularities or initial deformations [-] |
| $H_R$ | rigid part of relative oil film thickness [-] |
| $P$ | relative pressure [-] |
| $P_{cav}$ | relative cavitation pressure [-] |
| $P_G$ | relative pressure of feeding oil [-] |
| $R$ | shell radius [m] |
| $U$ | velocity of two relative moving surfaces [m.s$^{-1}$] |
| $\bar{U}$ | relative velocity [s$^{-1}$] |
| $A_F$ | complex compliancy matrix [N$^{-1}$m] |
| B | damping matrix [Nm$^{-1}$s] |
| J | Jacobian matrix [Nm$^{-1}$] |
| K | stiffness matrix [Nm$^{-1}$] |
| M | mass matrix [kg] |
| $Q_R$ | relative complex load matrix [N.m$^{-1}$] |
| $\alpha_p$ | mass proportional damping coefficient [s$^{-1}$] |
| $\beta_p$ | stiffness proportional coefficient [s] |
| $\gamma$, $\beta$ | Newmark´s algorithm coefficients [-] |
| $\Delta t$ | time step [s] |
| $\delta$ | angle of minimal oil film thickness [rad] |
| $\delta_R$ | penetration of surfaces [m] |
| $\mu$ | dynamic viscosity [Pa.s] |
| $\bar{\mu}$ | relative dynamic viscosity [-] |
| $\mu_0$ | dynamic viscosity at atmospheric pressure [Pa.s] |

$\psi$ matrix member distance from main diagonal [-]
$\rho$ oil density [kg.m$^{-3}$]
$\overline{\rho}$ relative oil density [-]
$\rho_0$ oil density at atmospheric pressure [kg.m$^{-3}$]
$\omega$ angular velocity in $z$ coordinate [rad.s$^{-1}$]
$\omega_{EQ}$ under-relaxation coefficient [-]
$\omega_{SOR}$ over-relaxation coefficient [-]
$\omega_x$, $\omega_y$ angular velocity in $x$ and $y$ coordinates [kg.m$^{-3}$]
$\varphi$ angular coordinate around pin [rad]
$\tau$ shear stress [Pa]
$\sigma$ combined surface roughness [m]
$\overline{\sigma}$ relative combined surface roughness [m.s$^{-2}$]
$\phi_x$, $\phi_z$ pressure flow factors [-]
$\phi_s$ shear flow factor [-]
$\phi_f$ shear stress factor due to sliding velocity [-]
$\phi_{fp}$ shear stress factor due to mean pressure [-]
$\phi_{fs}$ shear stress factor due to local roughness [-]

## REFERENCES


[1] G. Stachowiak and A. Batchelor, *Engineering tribology*. Oxford: Butterworth-Heinemann, 4th ed., 2014.

[2] H.J. Butenschön, 'Das hydrodynamische, zylindrische Gleitlager endlicher Breite unter instationärer Belastung', *PhD thesis*, Universität Karlsruhe, Germany, 1976.

[3] P. Novotný, 'Virtual Engine – A Tool for Powertrain Development', *Inaugural dissertation*, Brno University of Technology, Czech Republic, 2009.

[4] B. Jacobson and L. Floberg, *The finite journal bearing considering vaporization*, Technical Report 190, Institute of Machine Elements, Chalmer University of Technology, Gothenburg, Sweden, 1957.

[5] H.G Elrod, 'A cavitation algorithm', *Journal of Tribology*, vol. 103, pp. 350–354, 1986.

[6] S. Thomas, 'Analyse des Betriebsverhaltens von Kurbelwellengleitlagern mittels TEHD-Berechnungen', *PhD thesis*, RWTH Aachen, Germany, 2007.

[7] V. Čaika, S. Bukovnik G. Offner and W.J. Bartz, '*Elasto-hydrodynamic journal bearing model with pressure, temperature and shear rate dependent viscosity*, in *AITC-AIT 2006 International Conference on Tribology*, Parma, Italy, 2006.

[8] J. Javorova, A. Mazdrakova, I. Andonov and A. Radulescu, 'Analysis of HD Journal Bearings Considering Elastic Deformation and Non-Newtonian Rabinowitsch Fluid Model', *Tribology in Industry*, vol. 38, No. 2, pp. 186-196, 2016.

[9] Y. Okamoto, 'Numerical analysis of lubrication in a journal bearing by a thermoelastohydrodynamic lubrication (TEHL) model', *International Journal of Engine Research*, vol. 6, pp. 95–105, 2005.

[10] O. Marsalek, 'Advanced Methods for slide bearing dynamics solution', *PhD thesis*, Brno University of Technology 2015, Czech Republic.

[11] N. Patir and H. Cheng, 'Application of Average Flow Model to Lubrication between Rough Sliding Surfaces', *Journal of Lubrication Technology*, vol. 101, pp. 220–229, 1979.

[12] C. Arcoumanis, P. Ostovar and R. Mortier, 'Mixed Lubrication Modelling of Newtonian and Shear Thinning Liquids in a Piston-Ring Configuration', *SAE paper 972924*, 1997.

[13] J.A. Greenwood and J.H. Tripp, 'The Contact of two Nominally Flat Rough Surfaces', *Proceedings of the Institution of Mechanical Engineers*, vol. 185, pp. 625–633, 1970.

[14] H. Pasaribu and D. Schipper, 'Application of a Deterministic Contact Model to Analyze the Contact of a Rough Surface against a Flat Layered Surface', *Journal of Tribology*, vol. 127, pp. 451–455, 2005.

[15] M.B. Amor, S. Belghith, S. Mezlini, 'Finite Element Modeling of RMS Roughness Effect on the Contact Stiffness of Rough Surfaces', *Tribology in Industry*, vol. 38, No. 3, pp. 392–401, 2016.